PREDIS

Deliverable 4.10
Effect of irradiation on the durability of magnesium phosphate cement

Date 28.6.2024 Version Final

Dissemination Level PUBLIC

Ilaria Moschetti
IMT Atlantique
4 rue Alfred Kastler
La Chantrerie BP 20722
44307 Nantes cedex 3 – FRANCE

moschett@subatech.in2p3.fr

This project has received funding from the Euratom research and training programme 2019-2020 under grant agreement No 945098.

Project acronym PREDIS	Project title PRE-DISposal management of radioactive waste		Grant agreement No. 945098
Deliverable No. D4.10	Deliverable title Effect of irradiation on the durability of magnesium phosphate cement		Version Final
Type Report	Dissemination level PUBLIC		Due date M46
Lead beneficiary IMT			WP No. 4
Main author Ilaria Moschetti, IMT	Reviewed by Tomo Suzuki, IMT, Abdessalam Abdelous, IMT, WP4 Leader	Accepted by Maria Oksa, VTT, Coordinator	
Contributing authors POLIMI: Fabio Fattori, Eros Mossini, Andrea Santi, Gabriele Magugliani, Elena Macerata, Stefano Agosteo, Enrico Padovani, Mario Mariani; IMT: Abdesselam Abdelouas			Pages 24

Abstract

Deliverable 4.10 describes all the work and results achieved by the partners within the framework of T4.6.4 'Behaviour of magnesium phosphate cements under irradiation', namely the study of the behaviour under gamma irradiation of Magnesium Phosphate Cement (MPC), a direct conditioning solution for radioactive metal waste (RMW).

Keywords

Magnesium Phosphate Cement, Gamma Irradiation, Gas Release, Leaching Test, XRD, SEM-EDX, Compression Test, Freeze-Thaw Cycle

Coordinator contact

Maria Oksa
VTT Technical Research Centre of Finland Ltd
Kivimiehentie 3, Espoo / P.O. Box 1000, 02044 VTT, Finland
E-mail: maria.oksa.@vtt.fi
Tel: +358 50 5365 844

Acknowledgement

This project has received funding from the Euratom research and training programme 2019-2020 under grant agreement No 945098.

TABLE OF CONTENTS

LIST OF ABBREVIATIONS

COD
: Crystallography Open Database

CT
: Computed Tomography

EDF
: Électricité de France

EDX
: Energy Dispersive X-Ray

IC
: Ion Chromatography

ICP-MS
: Inductively Coupled Plasma - Mass Spectrometry

ICP-OES
: Inductively Copued Plasma - Optical Emission Spectroscopy

MPC
: Magnesium Phosphate Cement

OPC
: Ordinary Portland Cement

RMW
: Radioactive Metallic Waste

SEM
: Scanning Electron Microscope

WAC
: Waste Acceptance Criteria

XRD
: X-Ray Diffraction

μGC
: micro-Gas Chromatography

1 Introduction

The "PREDIS: Pre-Disposal Management of Radioactive Waste" initiative, launched by Euratom in September 2020, is a collaborative research and innovation endeavour spanning four years. Its primary objective is to advance the treatment and conditioning methods for low- and intermediate-level radioactive waste types presently lacking sufficient or industrially mature solutions. These waste categories encompass metallic materials, liquid organic waste, and solid organic waste. Moreover, the PREDIS project aims to innovate in the management of cemented waste and the evaluation of extended interim surface storage, employing digitalization solutions.

Work package 4 (WP4) of the PREDIS project addresses the lack of available technologies for Radioactive Metallic Waste (RMW) treatment and conditioning by investigating and developing innovative technologies for direct conditioning of RMW.

The work package is divided into different Tasks; Task T4.6 is dedicated to the encapsulation of reactive metals in Magnesium Phosphate Cements (MPC) based matrices. The main objective of this Task is to study the long-term performances of MPC.

This Deliverable is particularly focused on the work of Sub-task T4.6.4 – Behaviour of Magnesium Phosphate Cements under irradiation. Gamma irradiation was chosen to study the durability of this matrix because it is the most penetrating form of radiation and because of the radiation levels expected by RMW.

The list of partners involved in T4.6.4 describing the type of partner organization and its involvement is presented in Table 1.

Table 1: List of partners involved in PREDIS Sub-task T4.6.4.

Project partner		Country	Type of organization
Abbreviation	**Full Name**		
IMT	Institut Mines Télécom Nantes	France	University
POLIMI	Politecnico di Milano	Italy	University

1.1 Objective

This Technical report is the result of the Sub-task T4.6.4 created with an objective of filling the gap in the literature regarding the capabilities of MPC under irradiation and validating the matrix according to Waste Acceptance Criteria (WAC) requirements.

1.2 Structure of the report

The structure of the report is divided into three main parts. The first and second parts are devoted to the presentation of the experimental results (including the characterisation before and after irradiation) from IMT and POLIMI, respectively; the third part is composed of cross comparison between the two partners results.

2 Preparation of samples

MPC samples were prepared using the formulation reported in Table 2 and proposed by Chartier et al. [1].

Table 2: MPC formulation for one litre of mortar and raw materials' suppliers [1].

Material	Mass (g)	Supplier
MgO	131.39	Martin Marietta Magnesia Specialities
KH_2PO_4	443.58	YARA
Sand	574.97	Sibelco
Fly ash	574.97	Électricité de France (EDF)
H_3BO_3	11.50	
Water	293.24	

The mixture was prepared by starting to pre-mix the dry powders, which included MgO, KH2PO4, sand and fly ash. Next, boric acid was dissolved in water, ensuring that it dissolved completely and the solution returned to room temperature. Once the boric acid solution was ready, the premixed dry powders were gradually added to it. The combined ingredients were mixed at low speed for five minutes with a standardized mixer.

The IMT analyses were performed on cubic samples of 1.3 cm per side (Figure 1), kept in a 100% RH environment from casting to the start of irradiation.

POLIMI samples were prepared in a different geometry and size, i.e. equilateral cylinders of 5 cm, as reported in Figure 1. In addition, the mortars contained four contaminants, based on radionuclides normally found in nuclear wastes, added as analytical-grade nitrates of cobalt, strontium, caesium, and europium. Cobalt represented both Co-60, a common radionuclide in irradiated metallic alloys, and transition metals. Strontium and caesium, representing Cs-137 and Sr-90 fission products, additionally allowed to ascertain the behaviour of 1st and 2nd group elements within the MPC matrix. Lastly, europium, a lanthanide representative, was comprised since some of its isotopes, such as Eu-152 and Eu-154, are usual fission and activation products. The selected salts were dissolved in the water and boric acid solution; since nitrates are highly soluble in water, no precipitates were observed.

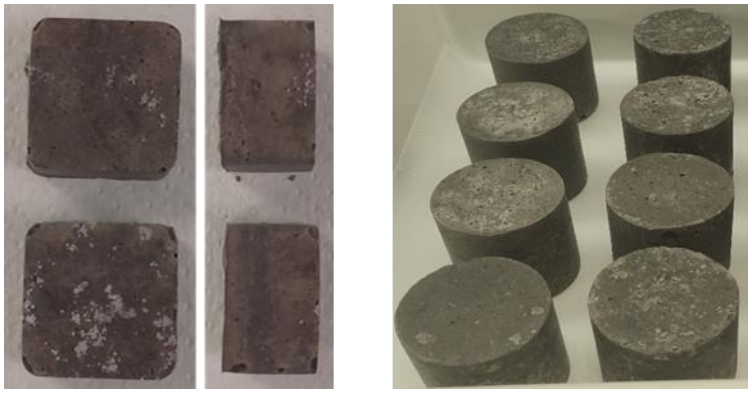

Figure 1: MPC cubic samples from IMT (left) and cylindrical ones from Polimi (right).

3 IMT Analyses

The detailed samples preparation and specification of the analyses performed are presented in Moschetti et al. (2023) [2].

3.1 Irradiation condition

Gamma irradiations (^{137}Cs) were performed at Arronax facility (Nantes, France). Dose rate was estimated around 400±80 Gy/h by Fricke dosimetry. Samples were irradiated between 6 days and 2 months to achieve total doses up to 200 kGy. The samples were placed in 22 mL sealed cylindrical PEEK cells (Figure 2). A glass tube with valve mounted on the cell enables connection for the gas measurement by micro-Gas Chromatography (μGC). After sealing, the cells were filled with Argon, to avoid the presence of O_2 and thus reproduce the anaerobic conditions that are expected in the deposit after about 50-100 years.

Figure 2: PEEK cell (left) and the gamma irradiator with Cs-137 radioactive source (right).

Each cell contained four samples of the same MPC batch spaced by a PEEK sample holder to avoid contact between the surfaces while ensuring gas movement, as shown in Figure 3. The presence of four samples also guaranteed a more representative gas yield, as the MPC samples are heterogeneous.

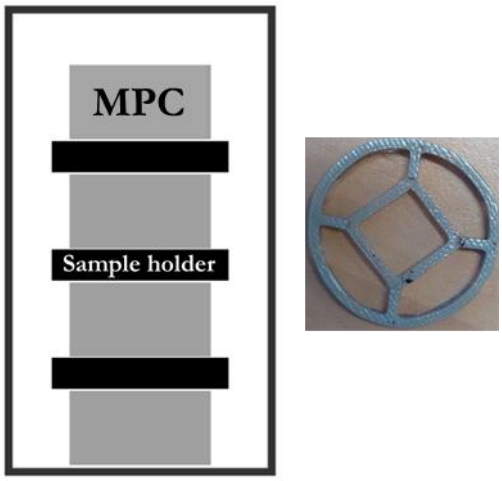

Figure 3: Representation of the set-up inside the irradiation cell (left) and sample holder top-view (right)

3.2 H_2 production

The gaseous atmosphere in the sealed cell was analysed using μGC (Agilent Technologie 490). The gas quantification was made considering the percentage of gas (in $\%vol$) determined by μGC, the gas pressure (P) after irradiation and the free volume V_{free} in the cells:

$$n(gas) = \frac{P \cdot \%vol \cdot V_{free}}{R \cdot T} \quad (1)$$

where R is the gas constant and T the sample temperature.

The moles of H_2 release and reported in Figure 4, each point is given by the average of 3 cells irradiated under the same conditions. The measure was performed on samples that started irradiation at different curing time and irradiated up to 200 kGy to better follow the H_2 release on a real case scenario.

The values at 1 day and 3 days of curing are around 6.4×10^{-7} mmol/kg, while the value at 14 days is lower, around 4.3×10^{-7} mmol/kg; however, all are inside the error bar of the last point at 28 days, equal to $(5 \pm 2) \times 10^{-7}$ mmol/kg. This slighter variation could be related to the longer curing time and thus a water stabilization and harder matrix. Nevertheless, the difference in moles between the samples with 1 day and 28 days of curing is not large enough to consider the fresh matrix significantly more sensitive to irradiation and useless for potential application.

In a previous work where gamma irradiation (^{60}Co – 900 Gy/h) was used on the same formulation, a H_2 release of 3.2×10^{-7} mmol/kg was measured [1]. In another former study, where a pure mix of magnesium oxide and potassium dihydrogen phosphate was irradiated (^{60}Co – 4.5 kGy/h), a H_2 release of 8.2×10^{-7} mmol/kg was measured [3]. Hence, the obtained values are in the same order of magnitude with the ones in literature.

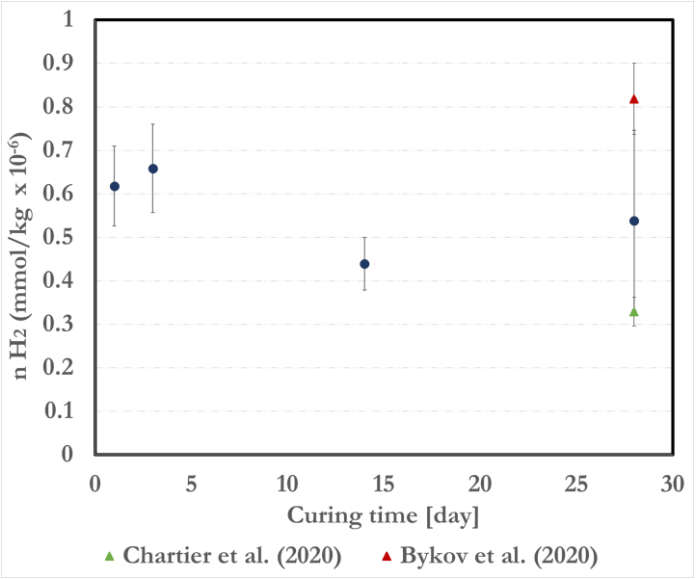

Figure 4: Hydrogen release after a total dose of 200 kGy vs curing days on which the samples were placed in the irradiator. Literature data are also reported in the plot [1], [3]

Calculating the value normalised to the amount of water contained in the samples, assuming no evaporation occurred or that it was contained since the samples were kept in an environment of 100% RH since the beginning of irradiation, a G(H_2) of 0.25±0.02 mol/J was obtained. These values are close to those measured for ultrapure water under argon-saturated conditions presented by Crumière et al. [4], therefore it can be concluded that the release of H_2 is related to the radiolysis of water contained in the samples and there is no production from secondary processes.

3.3 Mineralogical and Microstructural Characterization

3.3.1 XRD

Crystalline phases were identified by X-Ray Diffraction (XRD) (D8 Advance Bruker) performed on matrix samples. The investigation was performed in samples irradiated up to 200 kGy starting from different curing times to investigate mineralogical transformation at the beginning of curing (Figure 5), and on samples cured for 28 days prior to irradiation at different total doses, to better compare with literature data (Figure 6).

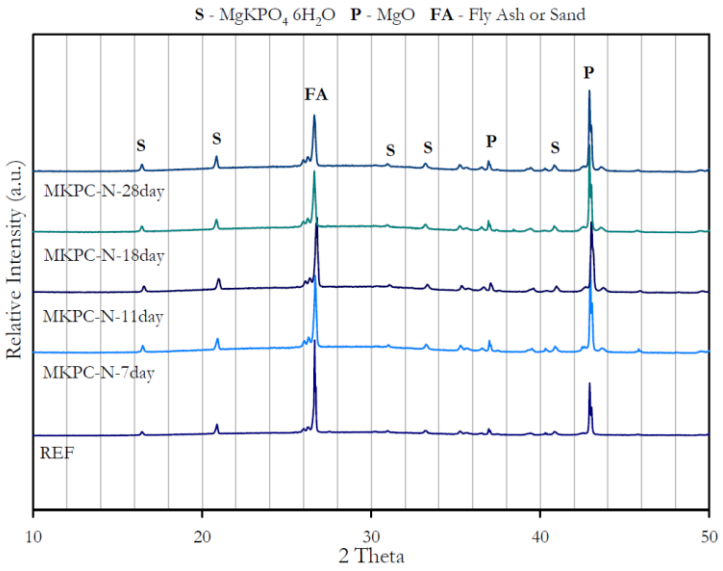

Figure 5: X-Ray pattern of MPC with same total absorbed dose (200 kGy) and different curing time. REF stands for non-irradiated sample.

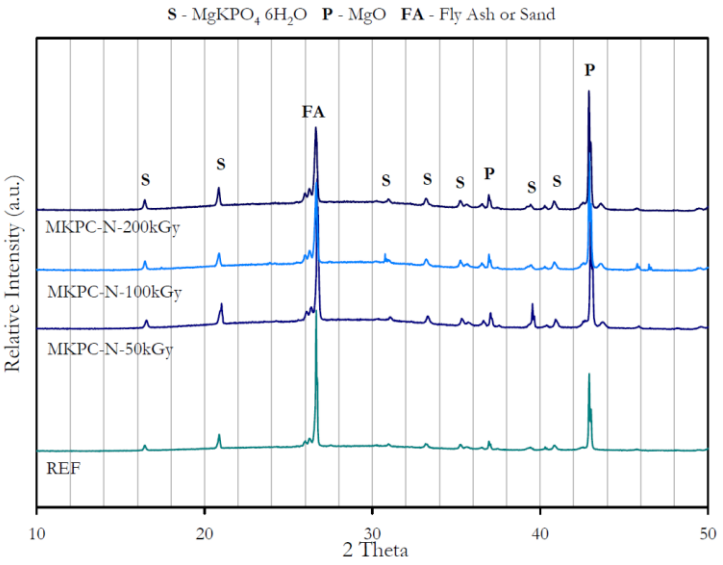

Figure 6: X-Ray pattern of MPC with same curing time (28 days) and different total absorbed dose. REF stands for non-irradiated sample.

The not irradiated MPC sample (REF), represented in both graphs, shows that the main phase is struvite-K ($MgKPO_4 \cdot 6H_2O$, Crystallography Open Database (COD) # 9010847). Traces of unreacted periclase (MgO, COD # 9006796), crystalline quartz (SiO_2 COD # 1011097) and mullite ($3Al_2O_3 \cdot 2SiO_2$, COD # 7105575) from fly ash are also identified.

The XRD patterns presented do not exhibit major changes considering the curing time (up to 28 days) and the total dose (up to 200 kGy) in comparison to the not irradiated sample and are also in agreement with previous works [1], [5].
These results confirm that irradiation does not produce measurable mineralogical changes and therefore supports the stability of this matrix for an application in the field of RMW encapsulation.
A further characterization was performed on MPC samples prepared with a variation of ± 5% on w/c ratio, namely water over MgO plus KH_2PO_4, and irradiated after 28 days of curing (Figure 7). This test was done to validate the formulation.

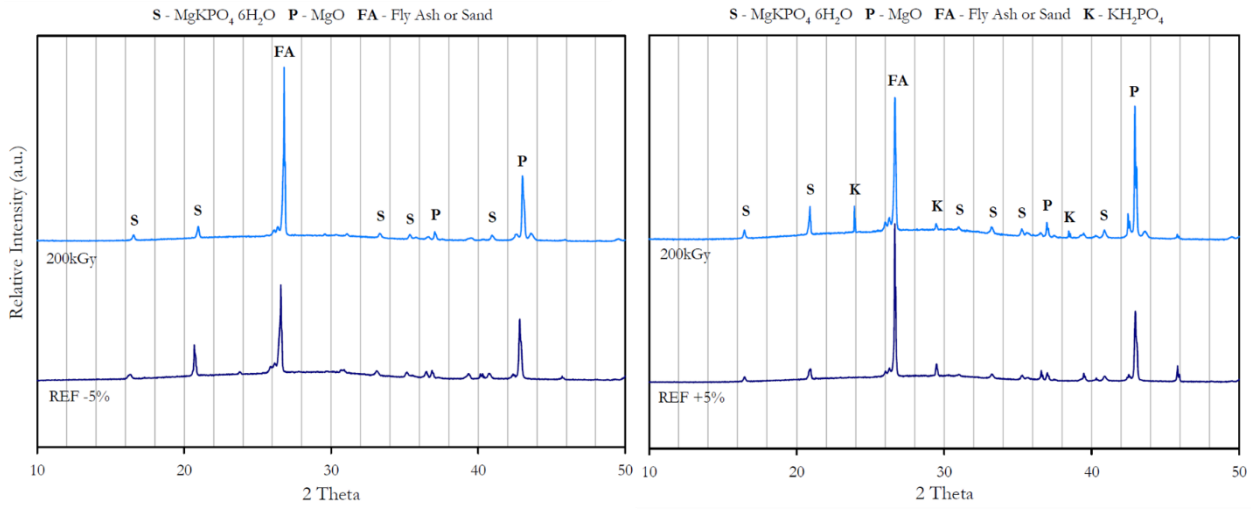

Figure 7: X-ray patterns of irradiated MPC samples with different w/c ratio, -5% w/c (left), +5% w/c (right).

The struvite-K phase is visible in the irradiated samples for both w/c ratio. Considering a possible industrialization of the process, the identification of the struvite-K promises a good robustness of the final phase even if variations in water content occur.

3.3.2 SEM-EDX

Scanning Electron Microscope (SEM) (JEOL JSM-5800LV) with Energy Dispersive X-Ray (EDX) (SAMx (NumeriX+)) were used to investigate the morphology of the samples as well as the chemical composition.
Sand grains and fly ash particles were found in all SEM scanning, in agreement with XRD results and previous works [6], [7]. Unreacted MgO phase was also discovered by EDX analyses in all samples, conforming to XRD measurements.
The composition of the struvite-K was evaluated by EDX and the Mg/P, Mg/K, and K/P molar ratios were calculated and presented in Table 3.
For the samples not subjected to irradiation, the molar ratios closely match the stoichiometric values (Mg/P = 1, Mg/K = 1, K/P = 1). However, irradiated samples exhibit a wider range of values in quantification. This variation could stem from detecting various morphologies of struvite-K, like needles or tabular crystals, as discussed in prior studies [8], [9], or from alterations induced by gamma irradiation.

Table 3: Struvite-K molar composition evaluated by EDX.

Sample		Mg/P	Mg/K	K/P
MPC	No Irr	1.18	1.26	0.94
	50 kGy	0.78 – 1.08	0.71 – 0.93	1.10 – 1.18
	200 kGy	0.65 – 3.7	0.36 – 3.6	1.02 – 1.8
-5%	No Irr	1.02	0.92	1.1
	200 kGy	0.52 – 0.96	0.5 – 0.84	1.04 – 1.14
+5%	No Irr	0.93	0.83	1.1
	200 kGy	1.04 – 1.4	1.44 – 1.5	0.72 – 0.94

3.4 Leaching Test

Leaching tests were performed according to the ANSI ANS 16.1 procedure [10].
The leaching solution, ultrapure water, was renewed at time intervals defined by the standard protocol and analysed to monitor changes in the release of matrix elements. The total duration of the test was 4 weeks. The Leachability Index (LI) was calculated for each element by:

$$LI = \frac{1}{n} \Sigma \left[log \left(\frac{\beta}{D_e} \right) \right]_n \quad (3)$$

where D_e is the effective diffusivity of the element [cm^2/s] and β is a constant equal to unity (1 cm^2/s). A material with an acceptable leaching resistance has a LI greater than 6, according to the Italian Inspectorate that is one of the strictest in Europe [11].
Three constitutive elements of the matrix were measured; Mg and K by Ion Chromatography (IC) (METROHM professional IC 850, column Metrosep C6 - 250mm/4mm), and Si by Single Quadrupole Inductively Coupled Plasma - Mass Spectrometry (ICP-MS) (XSERIES 2, ThermoFisher Scientific). Quantification of elements concentrations was based upon calibration curves prepared from single element standard solutions (SCP Science, Canada).
The investigation was performed in samples irradiated up to 200 kGy starting from different curing times to investigate mineralogical transformation at the beginning of curing (Figure 8), and on samples cured for 28 days prior to irradiation at different total doses, to better compare with literature data (Figure 10).

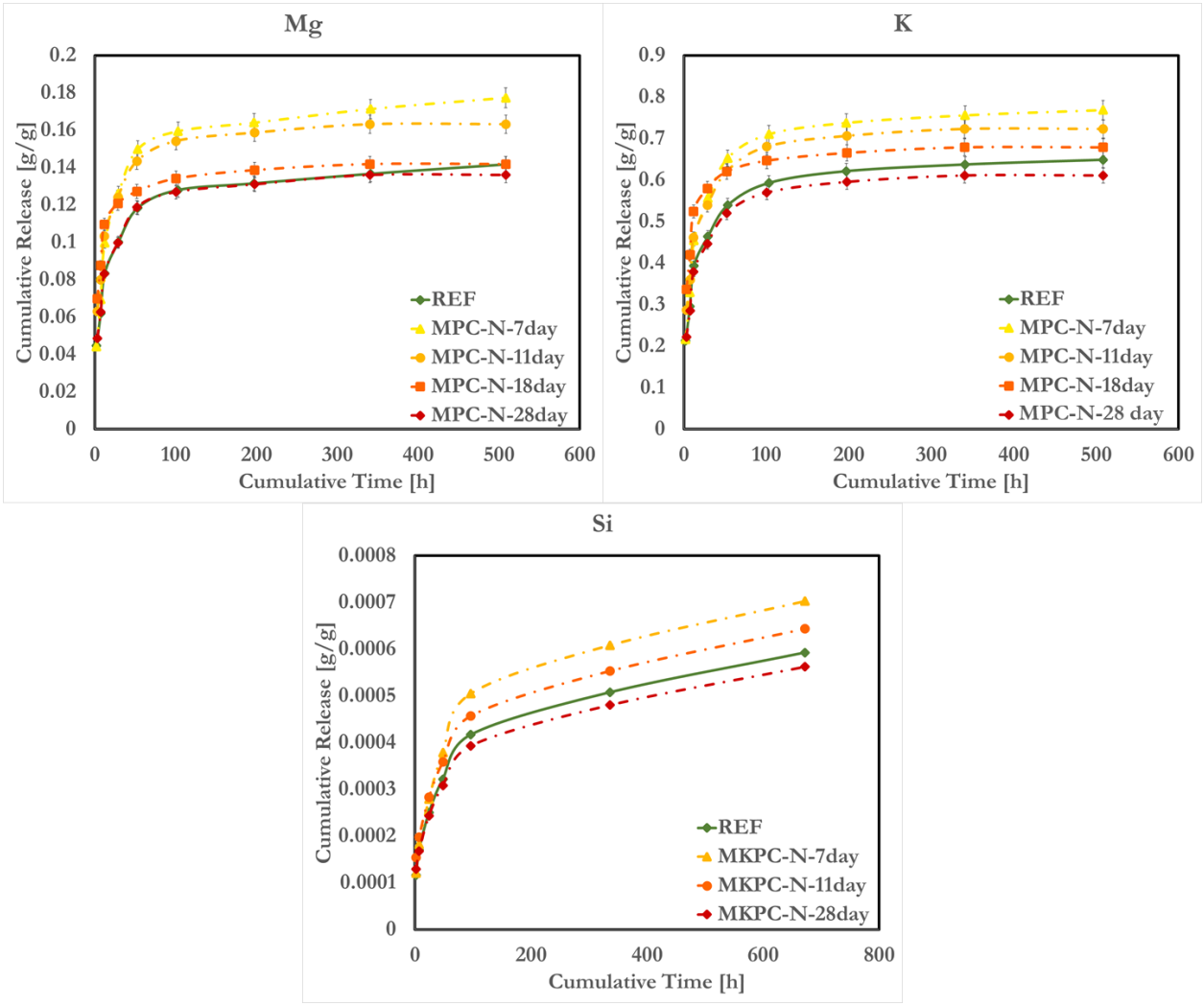

Figure 8: Cumulative leached ion concentration for MPC samples with same total dose (200 kGy) and different curing time.

The cumulative concentrations of Mg, K, and Si for MPC with the same total dose (200 kGy) shows for each element and for all analysed samples a stabilization of the values after 90 hours of immersion, and the LI calculated is also above 6 (Figure 9).

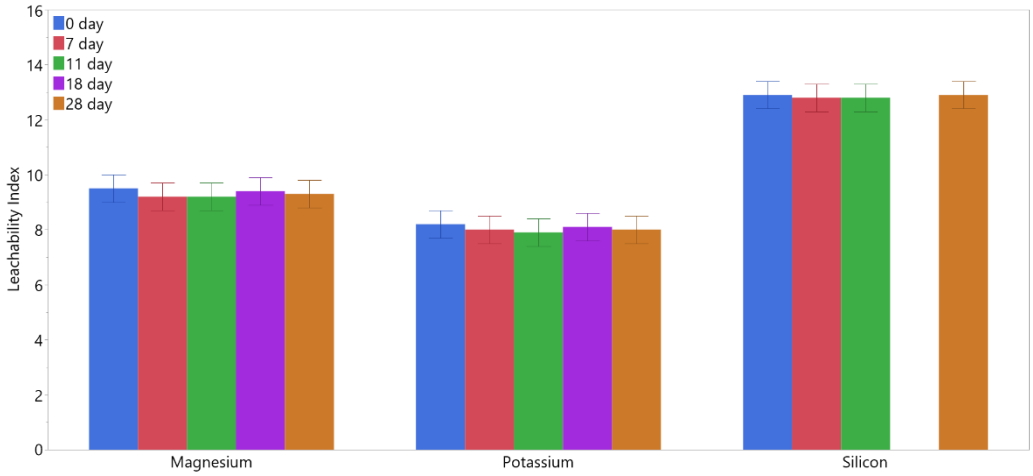

Figure 9: Intercomparison of the leachability indices of the main constituents for different curing time (uncertainty ±0.5). The Si for the samples cured for 18 days was not measured.

The observed trend suggests that as curing time increases, there is a decrease in the release of these elements. This phenomenon can be attributed to the matrix becoming more stable and impervious with longer curing times. Essentially, the increased curing time results in a denser and more tightly bound structure, which restricts the release of elements from the material.

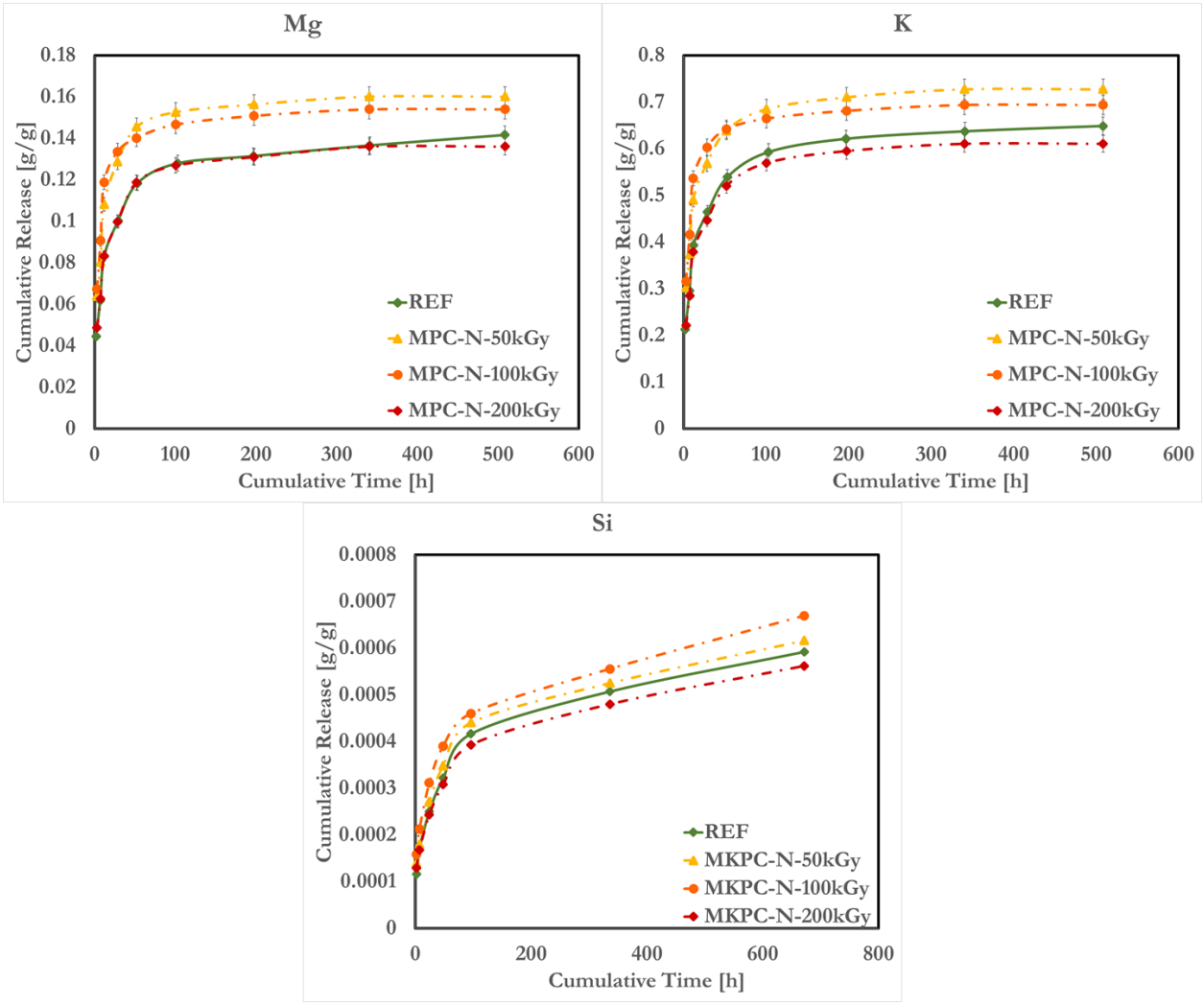

Figure 10: Cumulative ion concentration for MPC samples with same curing time (28 days) and different total absorbed dose.

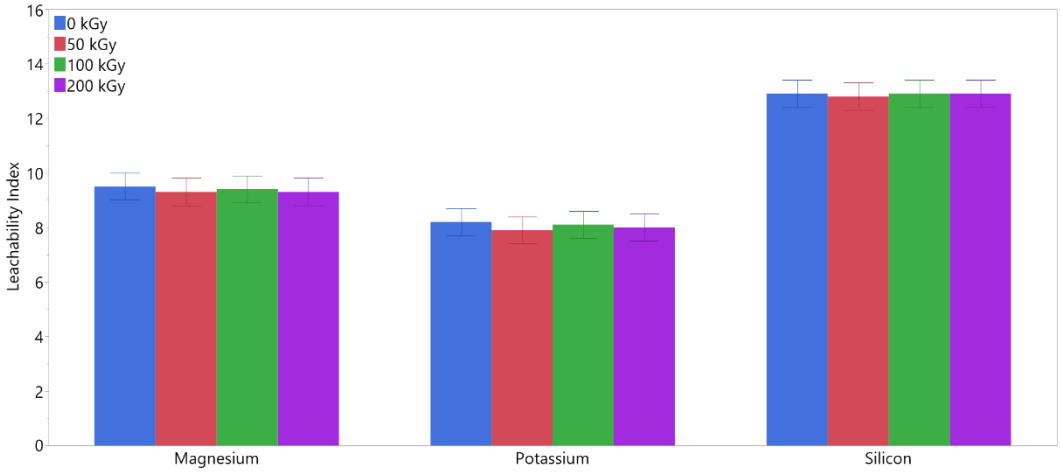

Figure 11: Intercomparison of the leachability indices of the main constituents for different total dose (uncertainty ±0.5).

The cumulative concentrations of Mg, K, and Si for MPC with the same curing time (28 days) shows the same stabilization behaviour of the samples above. The LI calculated is above 6 ensuring acceptable leaching resistance (Figure 11).
Analysing the trends depicted by the curves for the irradiated samples, it is revealed that a higher total dose correlates with a decrease in element release. Moreover, after 180 hours of immersion, the cumulative Mg concentrations appear to exhibit an inverse relationship with the dose rate, indicating that higher dose rates result in lower element release. Similar behaviour is observed for K after 380 hours of immersion, although not for Si.

A further characterization was performed on samples prepared with a variation of ±5% on w/c ratio and irradiated at 200 kGy after 28 days of curing (Figure 12).

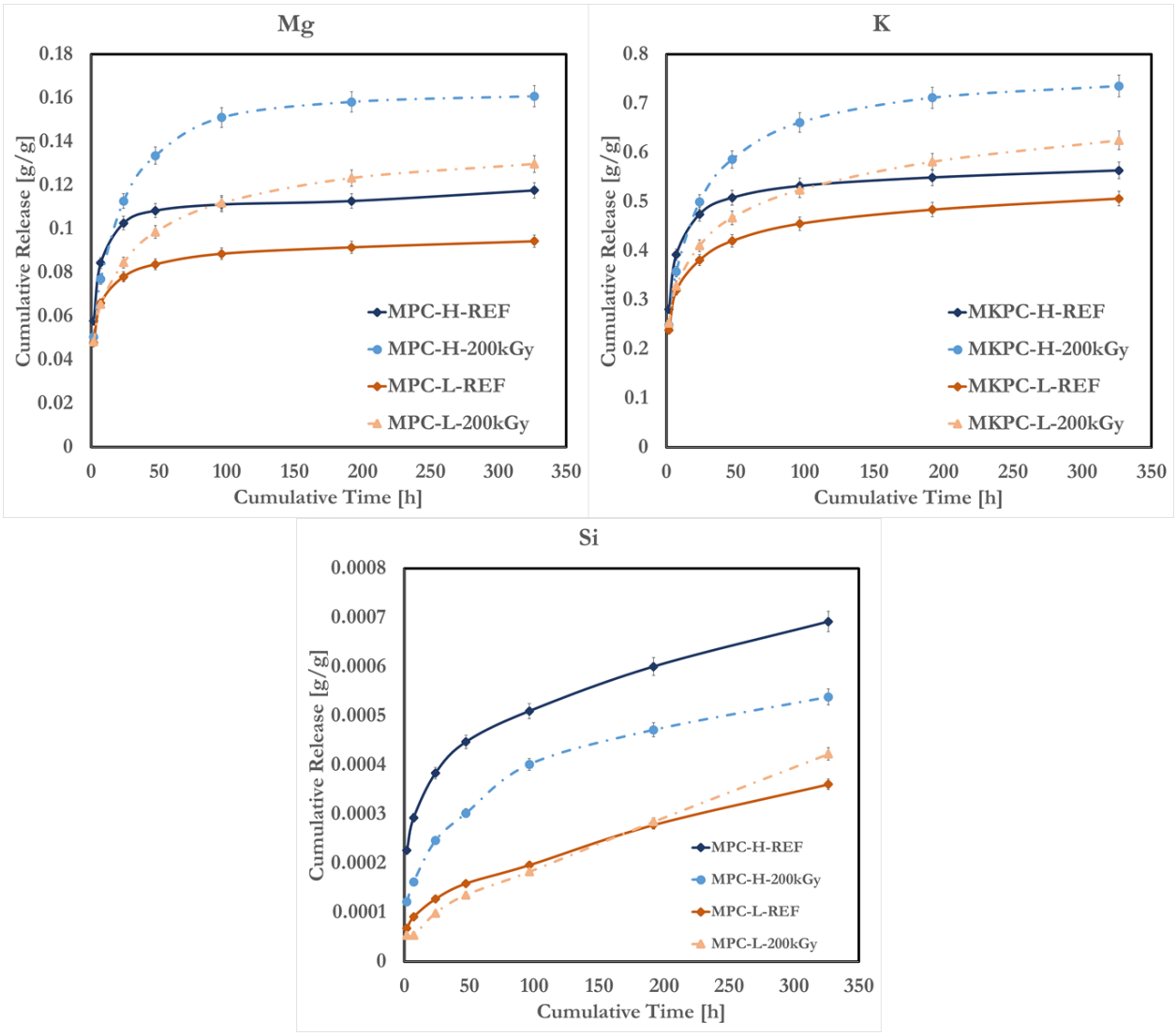

Figure 12: Cumulative ion concentration for MPC samples with different water content. L stands for -5% w/c, H for +5% w/c and REF for not-irradiated samples.

The cumulative concentrations of Mg, K, and Si for MPC with different water content shows the stabilization behaviour of Mg and K, but not the one of Si. However, the LI calculated is above 6 ensuring acceptable leaching resistance (Figure 13). Examining the patterns illustrated by the Mg and K curves, it's show that irradiated samples consistently exhibit higher release rates compared to non-irradiated ones. The behaviour of Si, however, deviates from this trend, but its release rates being orders of magnitude lower than those of Mg and K.

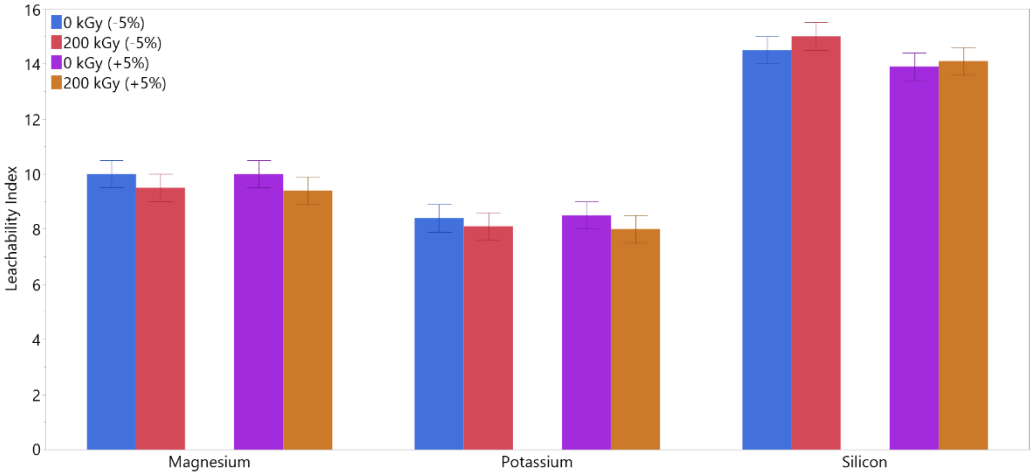

Figure 13: Intercomparison of the leachability indices of the main constituents for samples with different water to cement ratio (uncertainty ±0.5).

4 POLIMI Analyses

4.1 Irradiation condition

Samples were irradiated with an industrial Co-60 irradiator at a constant dose rate of 2.5 kGy/h. Cumulative absorbed doses of 200, 500, and 1000 kGy were chosen to investigate possible radiation-induced effects. After irradiation, a preliminary visual inspection gave no evidence of structural degradation, such as fractures, cracks, or chips. Additionally, no macroscopic signs of swelling or shrinkage were perceived.

4.2 Leaching Test

The 90-days three-dimensional leaching tests were conducted in osmotic water at controlled temperature (22 ± 1 °C) based on the ANSI/ANS-16.1-2019 protocol [10]. The investigation of possible immersion-induced effects is discussed in Sections 4.3 and 4.4. An overall examination of the samples confirmed the absence of macroscopic alterations or damage during the immersion period, as seen in Figure 14.

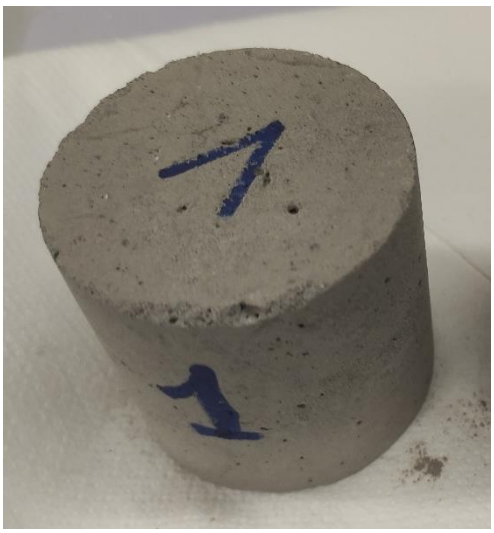

Figure 14: MPC sample at the end of the 90-days leaching test

The leaching process involves samples irradiated at 200, 500, and 1000 kGy, plus a non-irradiated blank sample for intercomparison. The analytes of interest are the main constitutive elements of the matrix, namely magnesium, phosphorus, and potassium, as well as the four added contaminants, i.e. caesium, strontium, cobalt, and europium. A preliminary analysis of the leachates' pH and conductivity was performed. The increase in pH shown in Figure 15 can be explained by the dissolution of MgO, which causes an increase of OH^- ions in solution. The noticeable increase in electric conductivity shown in Figure 16 is instead linked to the release of ionic species coming from the pore solution, in particular K^+. The concentration of the matrix constitutive elements inside the leachate was then measured using an ICP-OES, while regarding the contaminants ICP-MS was required thanks to its lower detection limit. For the analysis, the leachates were acidified using a 67% wt ultrapure HNO_3 solution and duly diluted afterwards for analysis using a 1% wt ultrapure HNO_3 solution.

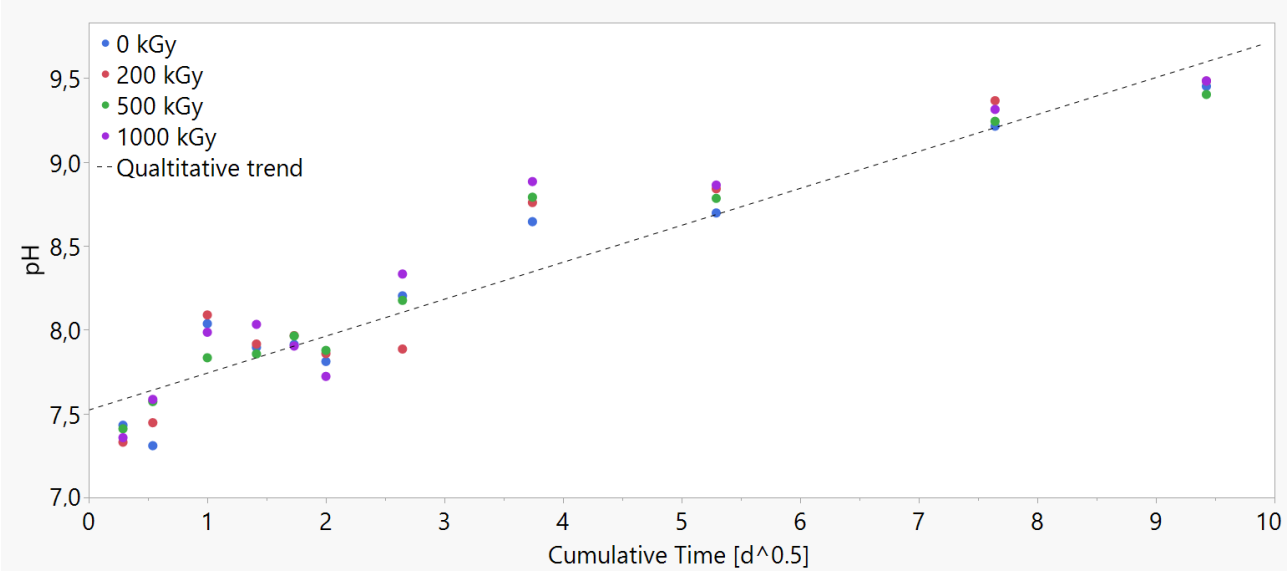

Figure 15: Leachates' pH (uncertainty of ±0.5).

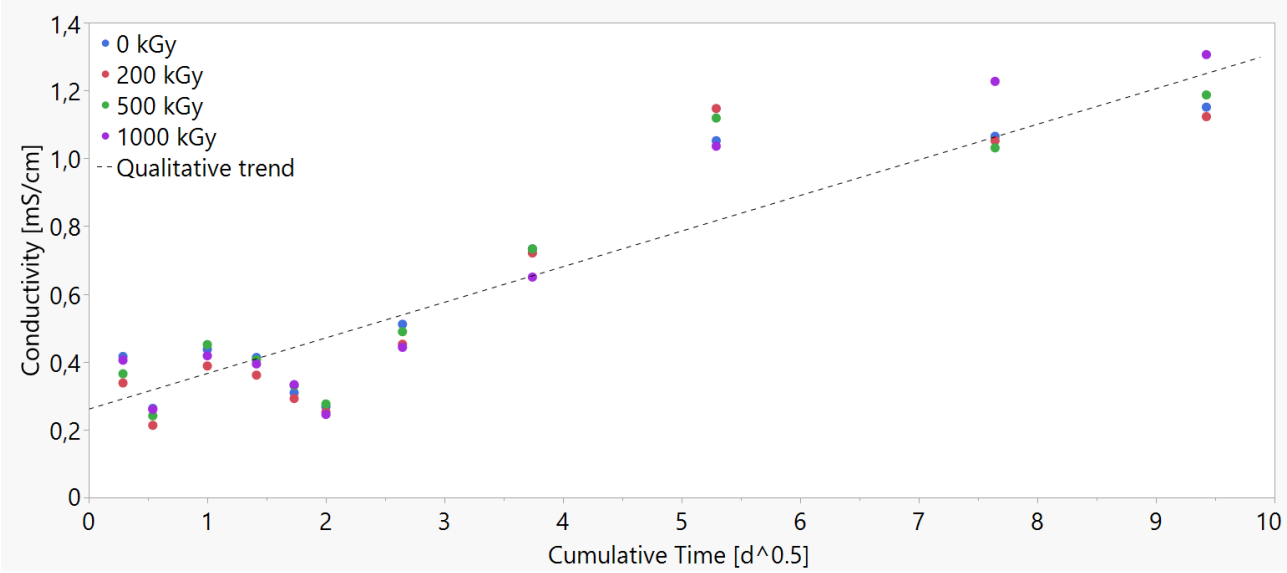

Figure 16: Leachates' conductivity (relative uncertainty of 4%).

The leachability indices for the main constituents are reported in Figure 17. No major radiation-induced changes can be assumed when compared to the non-irradiated blank sample, no matter the absorbed dose. The radiation stability of the MPC mortars for up to 1000 kGy is hence suggested, consolidating literature evidence [1], [3]. All samples exhibited analogous cumulative releases after

90 days of test; values in the order of 16 ± 1%, 7.0 ± 0.5%, and 2.0 ± 0.5% were measured for potassium, phosphorus, and magnesium, respectively.

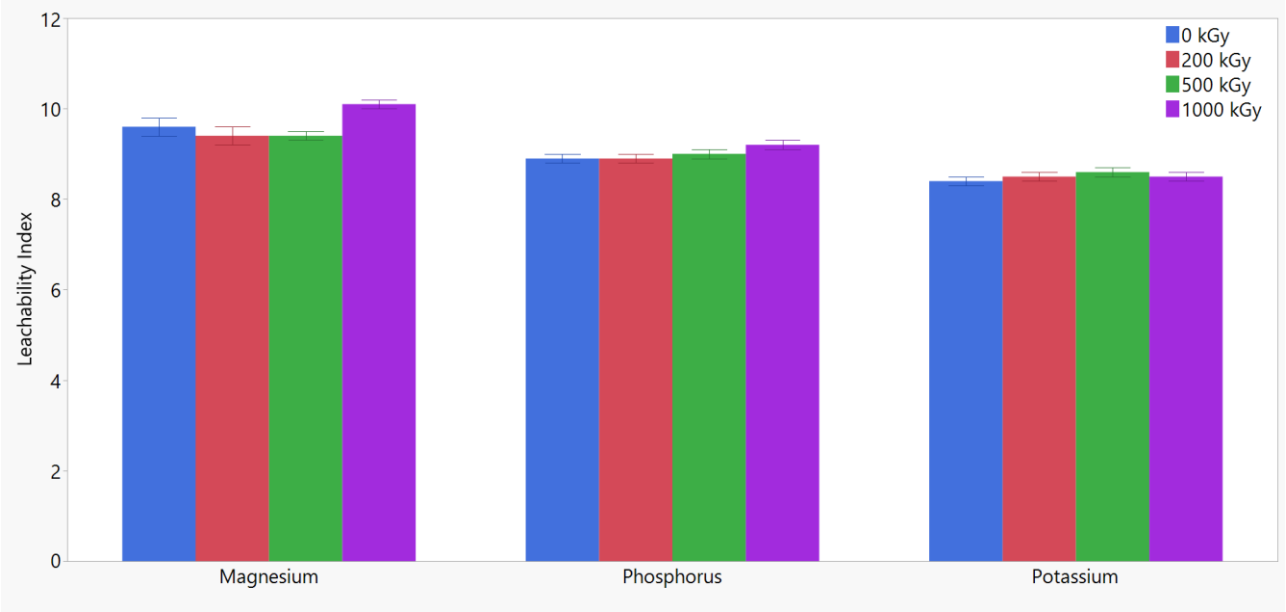

Figure 17: Intercomparison of the leachability indices of the main constituents for different doses.

The leachability indices of the four selected contaminants are displayed in Figure 18. As expected, considering its high mobility, caesium showed the weakest leaching behaviour. Cumulative releases of caesium after 90 days of test in the order of 5 ± 1% were measured, nonetheless to be considered a favourable outcome. Cobalt and strontium demonstrated similar leaching behaviours, giving rise to 90-days cumulative releases in the order of 1.0 ± 0.5%. Furthermore, the leachability indices of both contaminants remained comparable across different absorbed doses, supporting the hypothesis that irradiation had minimal influence. The leachability indices of europium are comparable to the non-irradiated blank sample, too. Minor amounts of Eu were leached (about 0.10 ± 0.05 % after 90 days) thanks to the low solubility of lanthanides in alkaline solutions [12]. The slight increase in LI, i.e. greater resistance to immersion, for samples irradiated up to 1 MGy, also shown in Figure 18, is probably due to the increased ageing of these samples due to the technical irradiation time.

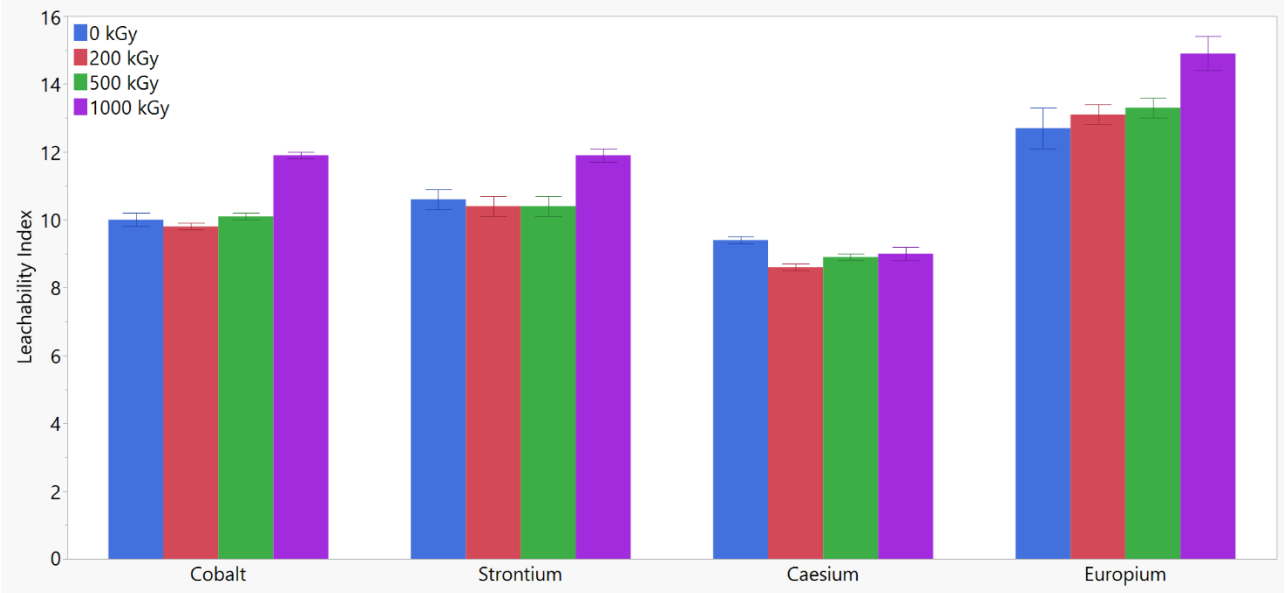

Figure 18: Intercomparison of the leachability indices of the contaminants for different doses.

4.3 Mineralogical and Microstructural Characterization

4.3.1 XRD

XRD was carried out with the following operating conditions: 2ϑ range from 4° to 80° and step size of 0.017°, monochromatized Cu-Kα radiation, 40 kV, 40 mA, counting time of 240 s per step. The analysis was performed on both leached and not leached 1000 kGy samples and compared to the non-irradiated ones. An intercomparison between the selected samples is reported in Figure 19. The patterns are almost identical. Generally speaking, since no meaningful variations are shown, the stability of the mineralogical phases under leaching and irradiation can be implied. It is possible to notice the mostly struvite-K and quartz crystalline structure of the mortars. Since high amounts of fly ash were used for this formulation, minor sillimanite and mullite phases were identified. The presence of unreacted MgO cannot be established because the periclase characteristic peaks almost coincide with those of mullite.

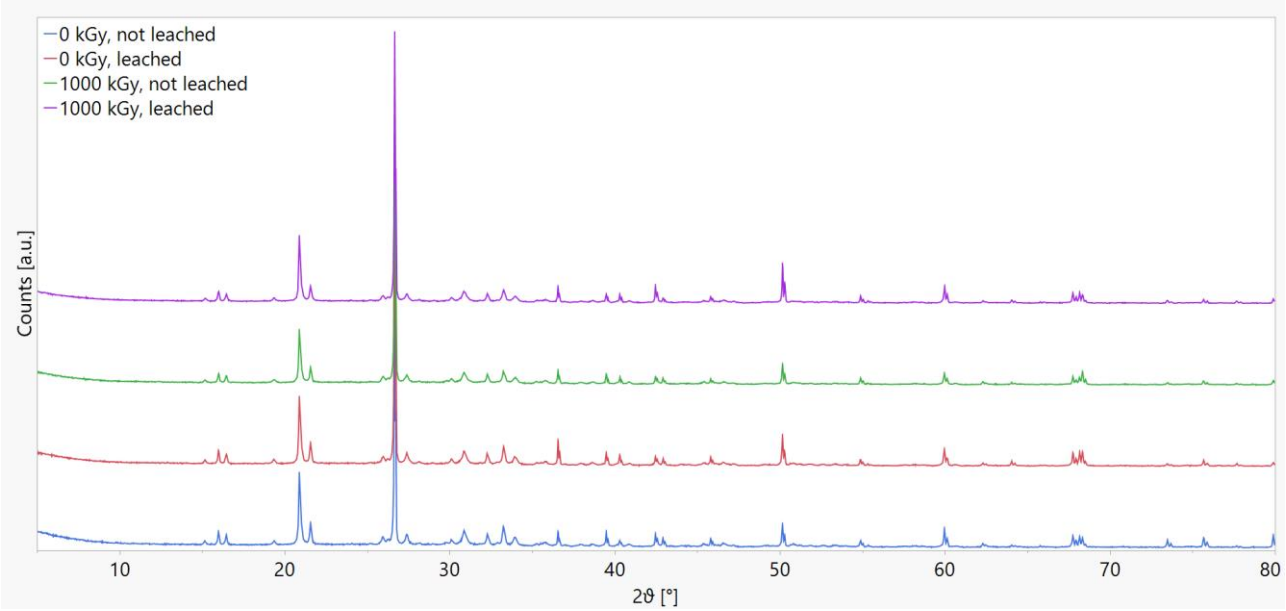

Figure 19: XRD patterns of the samples.

4.3.2 SEM-EDX and Micro-CT Analysis

To corroborate the obtained results, further investigations were carried out by SEM-EDX and Micro-CT on leached and not leached 1000 kGy samples and compared to the non-irradiated ones. No significant changes in morphology and microstructure were observed due to irradiation or immersion.

4.4 Compression Test

The compression tests were conducted following the UNI EN 12390-3:2019 protocol [13]. In order to mimic the damage caused on real waste forms by the flooding of the repository, the samples mentioned in Section 4.2 were compressed after a total of 90 days immersed in osmotic water. The results are shown in Figure 20. An uncertainty of 10% in the measurements is assumed due to several factors, namely the small dimension of the samples and minor non-uniformities such as small cavities. The mortars demonstrated high mechanical resistance, showing excellent behaviour to both lixiviation and irradiation up to 1000 kGy. All irradiated samples showed compression strengths similar to that of the non-irradiated one, as already reported in literature [1]. Moreover, at least 70% of the initial strength was retained after a 90-day leaching, a finding comparable to that of OPCs [14], [15], [16]. It is important to highlight that all the samples provided mechanical resistance far above the typical WAC requirements (as a reference, the Italian WAC for compressive strength is 10 MPa).

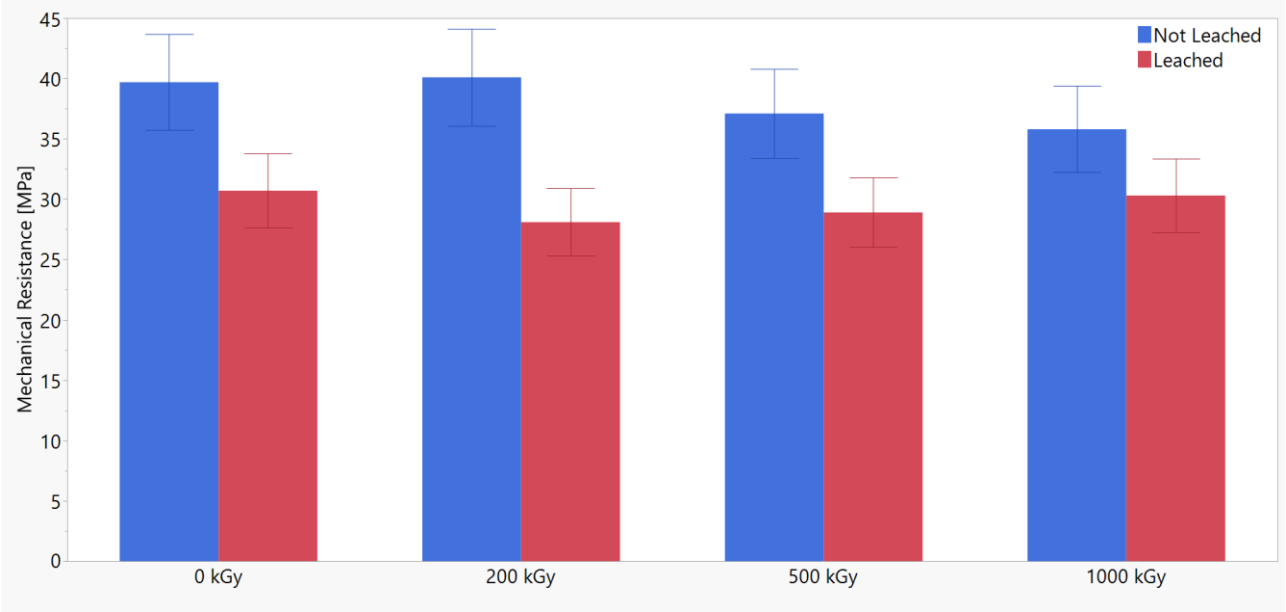

Figure 20: Mechanical resistance before and after 90 days of immersion for different doses.

4.5 Freeze-Thaw Cycles

The freeze-thaw cycles were conducted following the UNI 11193-2006 protocol [17] after which a compression test was carried out following the UNI EN 12390-3:2019 protocol [13]. The test consists of 30 cycles of temperature variations from -40 °C to +40 °C over a 24-hour period [13]. The test was performed on a unirradiated sample and compared with a sample subjected to a classical compression test. The tested specimen showed a loss of mechanical strength of approximately 12% compared to the direct compression test. This mechanical worsening may be caused by the expansion of the pore solution upon freezing, giving rise to greater internal hydraulic pressure that causes deterioration and, in the worst case scenario, fracturing of the cementitious matrix [18]. Additionally, thermal stresses arising from these cycles can build up, triggering changes in the structure and further deterioration [19], [20]. However, even after this ageing, the specimen satisfies the minimum compressive strength required by the Italian WAC, i.e. 10 MPa.

5 Discussion and Conclusion

The comprehensive study on the behaviour of MPC under gamma irradiation, conducted by both IMT Atlantique and POLIMI, presents promising findings for its potential application in radioactive waste management.

The measured hydrogen gas release, normalized to water content, showed values consistent with those reported in literature for similar materials, suggesting no significant secondary hydrogen production processes.

Leaching tests were conducted by both institutions, to assess MPC's leaching resistance under simulated repository conditions. Despite differences in samples irradiations and leaching parameters, both studies concluded that MPC exhibits favourable resistance to immersion, even after being exposed to high absorbed doses.

XRD and SEM-EDX analyses conducted by both institutions revealed the mineralogical stability of MPC under irradiation and leaching. Despite variations in sample preparation and irradiation conditions, both studies identified struvite-K as the main phase in MPC, indicating robustness in the cement matrix.

The compression tests performed by POLIMI to evaluate MPC's mechanical strength after irradiation and leaching, revealed that MPC maintained a high level of strength, with irradiated samples showing

mechanical characteristics that were comparable to those of non-irradiated samples This indicates that the mechanical performance of MPC was not adversely affected by radiation or leaching. Furthermore, experiments using freeze-thaw cycles demonstrate the robustness of MPC specimens, with mechanical resistance surpassing minimum regulatory standards post-aging.

In conclusion, while there are differences in experimental setups and methodologies between IMT Atlantique and POLIMI, the overarching findings demonstrate remarkable consistency in MPC's performance under irradiation and leaching. These similarities reinforce the robustness and reliability of MPC as a candidate for encapsulating radioactive waste, highlighting its potential for long-term nuclear waste management strategies.

REFERENCES

[1] D. Chartier *et al.*, “Behaviour of magnesium phosphate cement-based materials under gamma and alpha irradiation,” *Journal of Nuclear Materials*, vol. 541, p. 152411, Dec. 2020, doi: 10.1016/j.jnucmat.2020.152411.

[2] I. Moschetti, L. Sarrasin, G. Blain, E. Mossini, M. Mariani, and A. Abdelouas, “Effect of Curing Time and Water to Binder Ratio on Magnesium Potassium Phosphate Cement Exposed to Gamma Irradiation,” in *ASME 2023 International Conference on Environmental Remediation and Radioactive Waste Management*, Stuttgart, Germany: American Society of Mechanical Engineers, Oct. 2023, p. V001T05A001. doi: 10.1115/ICEM2023-109457.

[3] G. L. Bykov, V. A. Ershov, and B. G. Ershov, “Radiolysis of the magnesium phosphate cement on γ-irradiation,” *Construction and Building Materials*, vol. 252, p. 119156, Aug. 2020, doi: 10.1016/j.conbuildmat.2020.119156.

[4] F. Crumière, J. Vandenborre, R. Essehli, G. Blain, J. Barbet, and M. Fattahi, “LET effects on the hydrogen production induced by the radiolysis of pure water,” *Radiation Physics and Chemistry*, vol. 82, pp. 74–79, Jan. 2013, doi: 10.1016/j.radphyschem.2012.07.010.

[5] G. L. Bykov, E. V. Abkhalimov, V. A. Ershov, and B. G. Ershov, “Radiolysis of Portland cement and magnesium phosphate cement: Effect of the content and state of water on the Physicochemical properties and the mechanism and kinetics of hydrogen formation,” *Radiation Physics and Chemistry*, vol. 190, p. 109822, Jan. 2022, doi: 10.1016/j.radphyschem.2021.109822.

[6] Y. Li, T. Shi, and J. Li, “Effects of fly ash and quartz sand on water-resistance and salt-resistance of magnesium phosphate cement,” *Construction and Building Materials*, vol. 105, pp. 384–390, Feb. 2016, doi: 10.1016/j.conbuildmat.2015.12.154.

[7] M. R. Ahmad, B. Chen, and J. Yu, “A comprehensive study of basalt fiber reinforced magnesium phosphate cement incorporating ultrafine fly ash,” *Composites Part B: Engineering*, vol. 168, pp. 204–217, Jul. 2019, doi: 10.1016/j.compositesb.2018.12.065.

[8] L. J. Gardner, S. A. Bernal, S. A. Walling, C. L. Corkhill, J. L. Provis, and N. C. Hyatt, “Characterisation of magnesium potassium phosphate cements blended with fly ash and ground granulated blast furnace slag,” *Cement and Concrete Research*, vol. 74, pp. 78–87, Aug. 2015, doi: 10.1016/j.cemconres.2015.01.015.

[9] B. Xu, H. Ma, H. Shao, Z. Li, and B. Lothenbach, “Influence of fly ash on compressive strength and micro-characteristics of magnesium potassium phosphate cement mortars,” *Cement and Concrete Research*, vol. 99, pp. 86–94, Sep. 2017, doi: 10.1016/j.cemconres.2017.05.008.

[10] “Measurement of the leachability of solidified low-level radioactive wastes by a short-term test procedure.,” American Nuclear Society, La Grange Park, IL, American Nationa Standard, 2003.

[11] ISIN, “Criteri di sicurezza nucleare e radioprotezione per la gestione dei rifiuti radioattivi,” Ispettorato Nazionale per la Sicurezza Nucleare e la Radioprotezione, Guida Tecnica 33, Apr. 2023.

[12] R. Abdelrahman, A. Zaki, and A. Elkamash, “Modeling the long-term leaching behavior of 137Cs, 60Co, and 152,154Eu radionuclides from cement–clay matrices,” *Journal of Hazardous Materials*, vol. 145, no. 3, pp. 372–380, Jul. 2007, doi: 10.1016/j.jhazmat.2006.11.030.

[13] Ente italiano di normazione, “Methods of testing cement - Part 1: Determination of strength (UNI EN 196-1:2016).” May 19, 2016.

[14] A. Cheng, S.-J. Chao, and W.-T. Lin, “Effects of Leaching Behavior of Calcium Ions on Compression and Durability of Cement-Based Materials with Mineral Admixtures,” *Materials*, vol. 6, no. 5, pp. 1851–1872, May 2013, doi: 10.3390/ma6051851.

[15] J. S. Shon, G. Y. Kim, and J. Im, “Evaluation of efficient cementation of fission 99Mo production process waste and feasibility disposal of cement waste form,” *Annals of Nuclear Energy*, vol. 124, pp. 342–348, Feb. 2019, doi: 10.1016/j.anucene.2018.09.029.

[16] J.-S. Shon, H.-K. Lee, T.-J. Kim, G.-Y. Kim, and H. Jeon, “Evaluation of cementation of intermediate level liquid waste produced from fission 99Mo production process and disposal feasibility of cement waste form,” *Nuclear Engineering and Technology*, vol. 54, no. 9, pp. 3235–3241, Sep. 2022, doi: 10.1016/j.net.2022.03.033.

[17] Ente italiano di normazione, “Manufatti di rifiuti radioattivi condizionati - Metodi di prova per la qualificazione dei processi di condizionamento per manufatti appartenenti alla Categoria 2 (UNI 11193:2006).” Nov. 2006.

[18] H. Cai and X. Liu, “Freeze-thaw durability of concrete: ice formation process in pores,” *Cement and Concrete Research*, vol. 28, no. 9, pp. 1281–1287, Sep. 1998, doi: 10.1016/S0008-8846(98)00103-3.
[19] V. Penttala and F. Al-Neshawy, “Stress and strain state of concrete during freezing and thawing cycles,” *Cement and Concrete Research*, vol. 32, no. 9, pp. 1407–1420, Sep. 2002, doi: 10.1016/S0008-8846(02)00785-8.
[20] J. Guo, W. Sun, Y. Xu, W. Lin, and W. Jing, “Damage Mechanism and Modeling of Concrete in Freeze–Thaw Cycles: A Review,” *Buildings*, vol. 12, no. 9, p. 1317, Aug. 2022, doi: 10.3390/buildings12091317.